# Suppression of Spin Relaxation in Submicron InGaAs Wires

A. W. Holleitner,* V. Sih, R. C. Myers, A. C. Gossard, and D. D. Awschalom†

*Center for Spintronics and Quantum Computation, University of California, Santa Barbara, California 93106, USA*

(Received 6 February 2006; published 20 July 2006)

We investigate electron-spin dynamics in narrow two-dimensional *n*-InGaAs channels as a function of the channel width. The spin relaxation times increase with decreasing channel width, in accordance with recent theoretical predictions based on the dimensionally constrained D'yakonov-Perel' mechanism. Surprisingly, the suppression of the relaxation rate, which is anticipated for the one-dimensional limit, is observed for widths that are an order of magnitude larger than the electron mean free path. We find the spin precession length and the channel width to be the relevant length scales for interpreting these results.

DOI: 10.1103/PhysRevLett.97.036805 PACS numbers: 73.21.Hb, 71.70.Ej, 72.25.Dc, 85.75.Hh

In the emerging field of spintronics, it is important to explore carrier spin relaxation mechanisms in nanostructures as a function of dimensionality. The effect of reducing feature sizes in spintronic devices is relevant for future technological applications [1,2]. In two and three dimensions, elementary rotations do not commute, with significant impact on the spin dynamics if the spin precession is induced by spin-orbit coupling [3]. Spin-orbit coupling creates a randomizing momentum-dependent effective magnetic field; the corresponding relaxation process is known as the D'yakonov-Perel' (DP) mechanism [4]. In an ideal one-dimensional system, however, all spin rotations are limited to a single axis, and the spin rotation operators commute. In the regime approaching the one-dimensional limit, a progressive slowing and finally a complete suppression of the DP spin relaxation have been predicted, if the lateral width of a two-dimensional channel is reduced to be on the order of the electron mean free path [5–8]. The predictions are made for semiconductor heterostructures, such as InGaAs quantum wells (QW), in which the spin-orbit interactions are dominated by structural inversion asymmetry (SIA) [9–12]. Such solid-state systems have been proposed as candidates for spintronic devices, including spin transistors [13], due to their potential scalability and compatibility with existing semiconductor technology.

Here, we combine optical time-resolved Faraday rotation (TRFR) spectroscopy with magnetotransport measurements in two-dimensional, *n*-doped InGaAs QW channels. As a function of the channel width, we extract the spin relaxation time and the elastic scattering times of the electrons. Surprisingly, experiments on wide channels, with widths of an order of magnitude larger than the electron mean free path $l_e$, reveal an effective slowing of the spin relaxation. In this regime, the data show that the spin relaxation is dominated by the DP mechanism. For narrower channels, we find that an interplay between the spin precession length $l_{\mathrm{SP}}$ and the channel width $w$ determines the electron-spin dynamics in the wires. A saturation of the slowing spin relaxation is found for the narrowest wires, indicating other sources of spin relaxation exist such as the cubic spin-orbit coupling term due to bulk inversion asymmetry (BIA) [14] and the spin relaxation mechanism proposed by Elliot and Yafet [15].

The spin splitting in a QW due to SIA can be expressed in the form of an effective angular frequency vector

$$\mathbf{\Omega}(\mathbf{k}) = (1/l_{\mathrm{SP}})[\mathbf{v}(\mathbf{k}) \times \hat{z}] \tag{1}$$

with $\mathbf{k}$ the momentum vector, and $\mathbf{v}(\mathbf{k})$ the velocity of an electron [2]. $\hat{z}$ is the unit vector perpendicular to the QW, and $l_{\mathrm{SP}}$ is the spin precession length, over which the electrons remain spin polarized. Given a system with a fixed mean free path, a larger effective angular frequency induces faster spin rotations and, in turn, a shorter spin relaxation time. In the case of motional narrowing [16], the corresponding spin relaxation rate can be described as

$$\tau_{\mathrm{SP}}^{-1} = |\mathbf{\Omega}(\mathbf{k})|^2 \tau_M / 2 \tag{2}$$

with $\tau_M$ the momentum scattering time. In order to probe the spin dynamics for different momentum vectors, transport and spin coherence experiments are performed on a set of *n*-doped InGaAs wires [Fig. 1(a)]. Wires are patterned along the crystallographic directions [100], [110], [010], and $[\bar{1}10]$, while the spins are optically oriented along the growth direction [001]. Structures are fabricated by *e*-beam lithography and reactive ion etching out of three modulation-doped *n*-$In_{0.2}Ga_{0.8}As$/GaAs QW. The unpatterned QW A, B, and C have the following sheet densities $n_s$ and mobilities at a temperature of $T = 5$ K: (A) $5.4 \times 10^{11}$ cm$^{-2}$ and $3.8 \times 10^4$ cm$^2$/V s, (B) $6.6 \times 10^{11}$ cm$^{-2}$ and $3.1 \times 10^4$ cm$^2$/V s, and (C) $7.0 \times 10^{11}$ cm$^{-2}$ and $2.4 \times 10^4$ cm$^2$/V s. The QW are situated 100 nm below the surface of the heterostructures, and the QW width is $\Delta z = 7.5$ nm [for more details on the growth, see Ref. [17]]. The widths of the wires $w$ range between 420 nm and 20 $\mu$m, and the height of the wires is chosen to be 150 nm [Fig. 1(b)]. For the optical experiments, the wires are arranged in arrays with the dimension of $200 \times 200$ $\mu$m$^2$, while the diameter of the laser spot is about 50 $\mu$m. In order to provide constant etching parameters for all widths and directions of the wires, the distance between

 

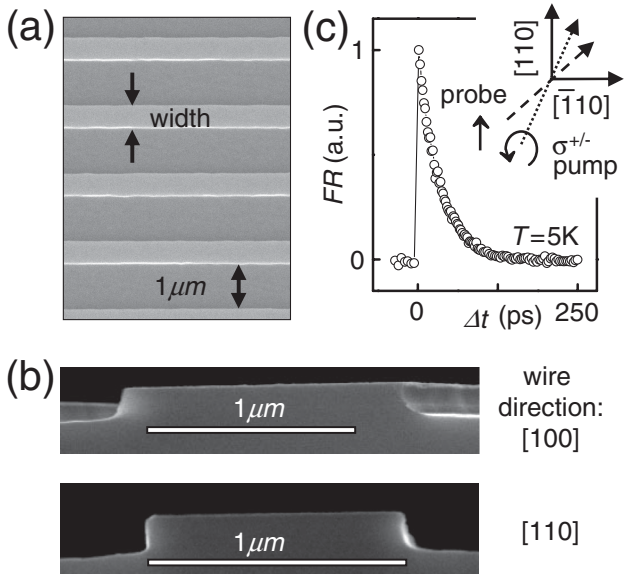


FIG. 1. (a) Scanning electron micrograph (SEM) of InGaAs channels. (b) SEM of sample A along the $[\bar{1}10]$ cleaving direction. Wires along [100] and [110] have a width of $(1.02 \pm 0.04)$ $\mu$m. (c) Faraday rotation of 750 nm wires patterned along [010] on sample A at zero magnetic field. Inset: a circularly polarized pump excites spin polarization, and a time-delayed linearly polarized pulse probes the spin dynamics.

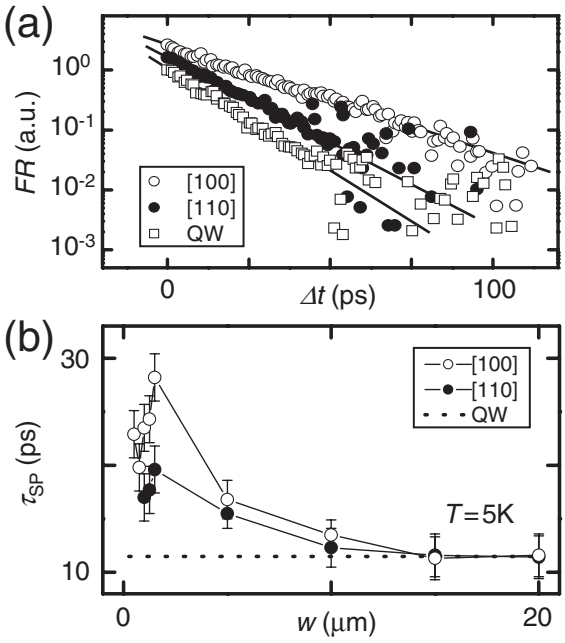


FIG. 2. (a) Faraday rotation at 5 K for sample B (open squares) and 750 nm wires patterned along [100] (open circles) and [110] (filled circles). Black lines are guides to the eye, and the data are offset for clarity. (b) Width dependence of spin relaxation times for wires fabricated from sample C. The dotted line depicts the spin relaxation time of the unpatterned QW. Measurements were performed at $B = 0$.

adjacent wires is set to be 1 $\mu$m for all of the arrays. Magnetotransport experiments are performed on single wires fabricated with the same etching parameters [18].

The electron-spin dynamics are probed with the TRFR technique, using 150 fs pulse trains from a mode-locked Ti:sapphire laser tuned to the absorption edge of the QWs; i.e. $E_{\mathrm{LASER}} = 1.35$ eV, 1.36 eV, and 1.37 eV for samples A, B, C [Fig. 1(c)] [17]. The evolution of the Faraday rotation angle can be described by a single exponential decay $\Theta_F = A_1 e^{-\Delta t/\tau_{\mathrm{SP}}}$ for all energies, where $A_1$ is the amplitude of the electron-spin polarization and $\Delta t$ is the time delay between the circularly polarized pump and the linearly polarized probe pulse. As shown with solid lines in Fig. 2(a), the exponential behavior of the data is described by a longitudinal spin relaxation time $\tau_{\mathrm{SP}}$ for both the unpatterned QW (open squares) and for the wires aligned along different crystallographic directions (data for sample B at 5 K and $P_{\mathrm{pump/probe}} = 400/150$ $\mu$W) [19]. For all samples, we find that at widths narrower than $\sim$10 $\mu$m, the spin relaxation times in the wires are longer than in the unpatterned QW [Fig. 2(b)] [20]. In addition, we find that wires aligned along [100] and [010] show equivalent spin relaxation times, which are generally longer than the spin relaxation times of wires patterned along [110] and $[\bar{1}10]$ (for clarity, only the data for the directions [100] and [110] are shown). All data are obtained by measuring the transmission signal in the Faraday geometry.

If an external magnetic field is applied perpendicular to the QW, the precession axis of the electron spin can be fixed independently of the scattered momentum vector. In the case that the DP mechanism is the dominant relaxation process, the following magnetic field dependence of the spin relaxation time has been predicted (for $\omega_C \tau < 1$) [21]:

$$\tau_{\mathrm{SP}}(B) = \tau_{\mathrm{SP}}(0)[1 + (\omega_C \tau)^2], \tag{3}$$

where $\omega_C = eB/m^*$ is the cyclotron frequency of an electron with charge $e$, $m^* = 0.064 m_e$ is the effective electron mass [17], and $\tau$ represents the intrinsic elastic scattering time. The magnetic field dependence of the spin relaxation time for the unpatterned QW is well fit by this prediction [Fig. 3(a), inset]. We find that $\tau \sim 1$ ps, in agreement with the measured momentum scattering time $\tau_M$ in these QW [17]. Figure 3(a) displays $\tau_{\mathrm{SP}}$ as a function of magnetic field for wires with $w = 1.25$ $\mu$m patterned on wafer C. The solid line shows the prediction according to Eq. (3) with a momentum scattering time of $\tau_M = (7.6 \pm 0.2) \times 10^{-13}$ s. In addition, we determine an estimate of the quantum lifetime $\tau_{\mathrm{QM}}$ through magnetotransport measurements on single wires by plotting the Shubnikov-deHaas oscillations in a Dingle plot [22]. Surprisingly, the optical data are better fit using the quantum lifetime $\tau_{\mathrm{QM}} = (3.1 \pm 0.1) \times 10^{-13}$ s [23] (dashed and dotted lines for the directions [100] and [110], respectively). Generally, the ratio between the momentum scattering time and the quantum lifetime gives a measure for the relative contribution of the large and small angle scattering mechanisms [24]. The

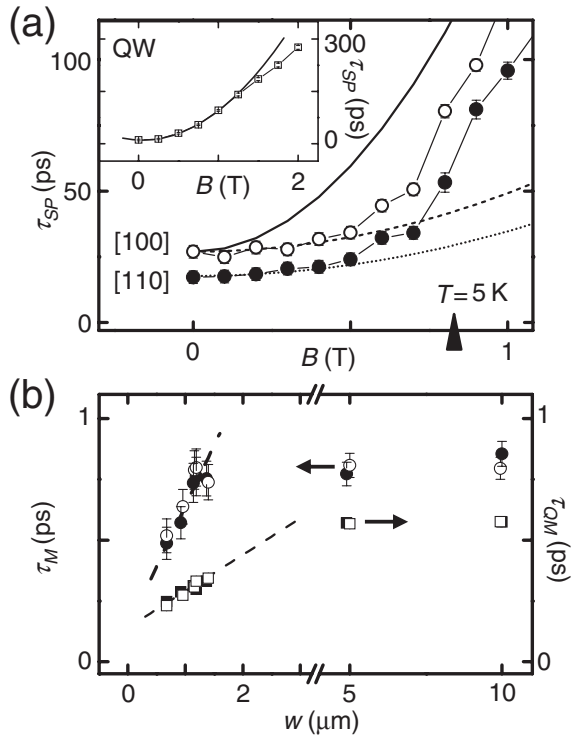


FIG. 3. (a) Magnetic field dependence of spin relaxation times in the unpatterned sample C (inset) and wires (open and filled circles for [100] and [110], respectively). The magnetic field is applied perpendicular to the surface of the sample. The dotted, dashed, and black lines are fits to Eq. (3), and the triangle indicates $B_{\mathrm{QM}}$ (see text for details). (b) Momentum scattering time (circles) and quantum lifetime (squares) vs channel width for the directions [100] (open symbols) and [110] (filled symbols), respectively. The dashed lines are guides to the eye.

condition $\omega_C \tau_{\mathrm{QM}} = 1$ can be represented by a magnetic field $B_{\mathrm{QM}} = m^*/e\tau_{\mathrm{QM}}$, which is depicted as a triangle. It can be nicely seen that Eq. (3) describes the data well for $\omega_C \tau_{\mathrm{QM}} < 1$. This field dependence of $\tau_{\mathrm{SP}}$ suggests that (i) the DP mechanism is indeed the dominant spin relaxation mechanism in the studied structures and (ii) the quantum lifetime $\tau_{\mathrm{QM}}$ is the relevant time scale for the wires at low magnetic field values where the Zeeman energy is negligible [23].

Figure 3(b) shows the dependence of $\tau_M$ and $\tau_{\mathrm{QM}}$ on the channel width. Both scattering times show a rapid decrease for the narrowest channels. Since the spin relaxation times greatly exceed the charge scattering times, the QW can be considered to be in the "motional narrowing" regime [Eq. (2)] [16]. Figure 3(b) further demonstrates that $\tau_M$ is constant for wires with $w \geq 1.2\ \mu$m, independent of the crystallographic direction [the value of the momentum scattering time corresponds to a mean free path $l_e = (275 \pm 5)$ nm]. In Fig. 2(b), however, we find an enhanced spin coherence for wires with $w \leq 5\ \mu$m. This implies that for $1.2\ \mu\mathrm{m} \leq w \leq 5\ \mu$m, the effective angular frequency $|\mathbf{\Omega}(\mathbf{k})|$ is reduced, according to Eq. (2). Experimentally we find that a temperature rise results in a decrease of the spin relaxation time in the channels (data not shown). Therefore, we can exclude dissipation effects in the wires [23]. At the same time, we observe from the images shown in Fig. 1(b) that the channels are homogeneously etched. Consequently, strain relaxation in the QW via dislocation nucleation is unlikely for wires with $1.2\ \mu\mathrm{m} \leq w \leq 5\ \mu$m and a QW width of $\Delta z = 7.5$ nm [25]. This interpretation is supported by the fact that $n_S$ shows no dependence on the channel width and direction down to $w \sim 400$ nm.

Figure 4(a) shows the ratio between the wire width $w$ and the spin diffusion length

$$l_{\mathrm{SD}} = \sqrt{\tau_{\mathrm{SP}} \cdot v_F^2 \tau_M / 2} \tag{4}$$

as a function of $w$ [7]. In the motional narrowing regime, the spin diffusion length is the same as the spin precession length; inserting Eq. (2) into Eq. (4) yields $l_{\mathrm{SD}} = v_F/|\mathbf{\Omega}(\mathbf{k})| = l_{\mathrm{SP}}$ [7]. For wide channels, the spin precession or diffusion length is given by the two-dimensional limit, i.e., a linear dependence of $w/l_{\mathrm{SP}}$ versus $w$ (dashed line). For narrow widths, however, the data suggest that the

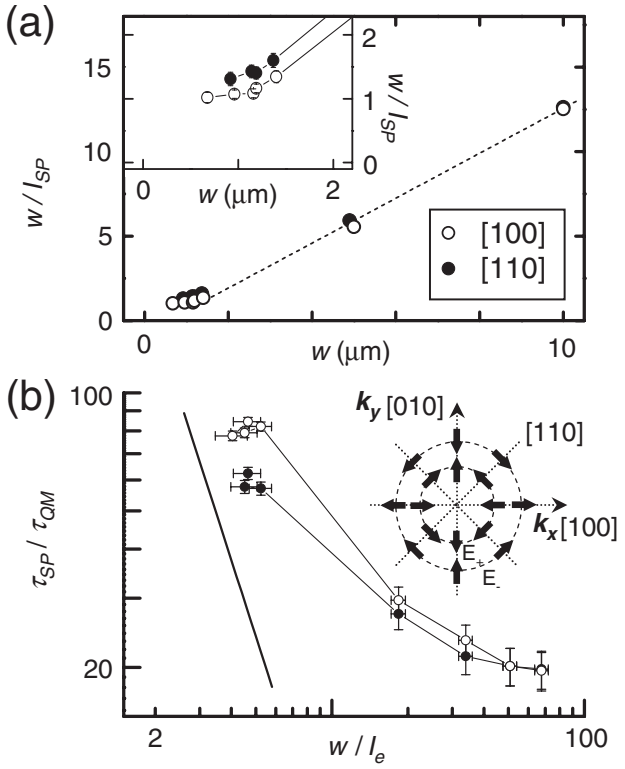


FIG. 4. (a) Ratio of the channel width $w$ and the spin diffusion length $l_{\mathrm{SP}}$ as a function of $w$. Inset: for narrow wires, the channel boundaries limit the spin diffusion length. (b) Logarithmic presentation of the spin relaxation time in units of the scattering time and the mean free length. Black line depicts the quasi-one-dimensional limit (open and closed circles for [100] and [110], respectively). Inset: schematic vector map of the spin eigenfunctions in a QW with bulk inversion asymmetry.

spin diffusion length is ultimately limited by the wire width ($w/l_{SP} \sim 1$) [Fig. 4(a), inset]. Concerning the spin diffusion length, the narrowest wires act as quasi-one-dimensional channels and, in turn, the two-dimensional spin dynamics are constrained by the side walls of the wires [5–8]. Figure 4(b) depicts the ratio of $\tau_{SP}$ and $\tau_{QM}$ as a function of the mean free path $l_e$ in a logarithmic scale. A qualitatively similar graph is obtained using $\tau_M$ instead of $\tau_{QM}$. The graph closely resembles the predictions of Ref. [7], which indicates that the slowing of the spin relaxation in the wires is due to a dimensionally constrained DP mechanism, as predicted for SIA [5–8]. The DP spin relaxation due to BIA eventually limits this slowing [6]. An anisotropy in the spin splitting and, thus, in $|\mathbf{\Omega}(\mathbf{k})|$ has been predicted for InGaAs QW assuming cubic BIA terms and Fermi wave vectors which are comparable to $k_F = \sqrt{2\pi n_S} \cong (0.018\text{–}0.021)$ Å$^{-1}$ of the discussed samples [14]. Since the spin splitting due to BIA is anisotropic, the magnitude of $|\mathbf{\Omega}(\mathbf{k})|$ depends sensitively on the momentum vector. This explains why spin lifetimes are similar for channels oriented along [100] and [010], but are different from wires patterned along the [110] and [$\bar{1}$10] directions. The inset of Fig. 4(b) depicts the orientation of the spin eigenfunctions for two spin-split subbands $E_+$ and $E_-$ of a zinc blende QW in the presence of BIA [$E_+$ and $E_-$ are defined as in Ref. [14] ]. For SIA, however, Eq. (1) suggests a constant value of $|\mathbf{\Omega}(\mathbf{k})|$ that only depends on the magnitude of $\mathbf{k}$ and which is always oriented perpendicular to $\mathbf{k}$. For the narrowest channels, the data do not reach the predicted behavior of $\tau_{SP} \sim w^{-2}$ [black line in Fig. 4(b)], where the channel width would limit the mean free path [6,7]. Instead, we find a saturation of the spin relaxation time. Since the Elliott-Yafet mechanism becomes more effective for shorter scattering times, this relaxation mechanism ultimately limits the slowdown of the spin relaxation in the narrowest channels [15].

Generally, we utilize InGaAs QW with a relatively low In concentration and an electron mobility $\mu \cong (2\text{–}4) \times 10^4$ cm$^2$/V s. The spin precession length $l_{SP} \cong (0.9\text{–}1.1)$ $\mu$m [Fig. 4(a)] yields a Rashba spin coupling constant of $\alpha \equiv \hbar^2/(2l_{SP}m^\star) \cong (0.5\text{–}0.7) \times 10^{-12}$ eV m [2,7], in good agreement with previous results on InGaAs QW [10,26]. This set of parameters ensures that the QW are in the "motional narrowing" regime, in order to detect the dimensionally constrained DP mechanism [5–8]. Coupling constants of $\alpha \cong 4 \times 10^{-11}$ eV m have been achieved by increasing the In concentration in the QW [9,11,13,26]. Larger coupling constants entail relatively short spin precession lengths and thus shorter spin relaxation times, which can be compensated by lowering the electron mobility.

In summary, an effective slowing of the D'yakonov-Perel' (DP) spin relaxation mechanism is observed in unexpectedly wide conducting channels of $n$-InGaAs quantum wires. For the narrowest wires with only a few hundreds of nanometers width, an interplay between the spin diffusion length and the wire width determines the spin dynamics.

We thank Y. Li for technical support and F. Meier, V. Khrapay, and J. P. Kotthaus for stimulating discussions. We gratefully acknowledge financial support by the AFOSR, DMEA, NSF, and ONR.

*Present address: Center for NanoScience (CeNS), Munich, Germany.
†Electronic address: awsch@physics.ucsb.edu

[1] S. A. Wolf *et al.*, Science **294**, 1488 (2001).
[2] *Semiconductor Spintronics and Quantum Computation, NanoScience and Technology*, edited by D. D. Awschalom, D. Loss, and N. Samarth (Springer-Verlag, Berlin, 2002).
[3] Y. Kato *et al.*, Nature (London) **427**, 50 (2004).
[4] M. I. D'yakonov and V. I. Perel', Zh. Eksp. Teor. Fiz. **60**, 1954 (1971) [Sov. Phys. JETP **33**, 1053 (1971)]; M. I. D'yakonov and V. Yu. Kachorovskii, Fiz. Tekh. Poluprovodn. **20**, 178 (1986) [Sov. Phys. Semicond. **20**, 110 (1986)].
[5] A. Bournel *et al.*, Eur. Phys. J. Appl. Phys. **4**, 1 (1998).
[6] A. G. Mal'shukov and K. A. Chao, Phys. Rev. B **61**, R2413 (2000).
[7] A. A. Kiselev and K. W. Kim, Phys. Rev. B **61**, 13 115 (2000).
[8] T. P. Pareek and P. Bruno, Phys. Rev. B **65**, 241305(R) (2002).
[9] J. Nitta *et al.*, Phys. Rev. Lett. **78**, 1335 (1997).
[10] T. Koga *et al.*, Phys. Rev. Lett. **89**, 046801 (2002).
[11] D. Grundler, Phys. Rev. Lett. **84**, 6074 (2000).
[12] S. D. Ganichev *et al.*, Phys. Rev. Lett. **92**, 256601 (2004).
[13] S. Datta and B. Das, Appl. Phys. Lett. **56**, 665 (1990).
[14] R. Winkler, Phys. Rev. B **69**, 045317 (2004).
[15] P. G. Elliott, Phys. Rev. **96**, 266 (1954); Y. Yafet, in *Solid State Physics*, edited by F. Seitz and D. Turnbull (Academic, New York, 1963), Vol. 13.
[16] W. H. Lau, J. T. Olesberg, and M. E. Flatté, Phys. Rev. B **64**, 161301(R) (2001).
[17] V. Sih *et al.*, Phys. Rev. B **70**, 161313(R) (2004).
[18] After patterning, $n_s$ is reduced by about $(17 \pm 1)$%, and the mobility is lowered by about $(5 \pm 5)$%.
[19] The longitudinal spin relaxation time is often denoted as "$T_1$."
[20] The error bars in the figures include a minor variation of the spin lifetime which can be detected if the laser power or the laser energy is altered.
[21] *Optical Orientation*, edited by F. Meier and B. P. Zakharchenya (Elsevier, New York, 1984).
[22] R. B. Dingle, Proc. R. Soc. A **211**, 517 (1952).
[23] M. A. Brand *et al.*, Phys. Rev. Lett. **89**, 236601 (2002).
[24] S. Das Sarma and F. Stern, Phys. Rev. B **32**, 8442 (1985).
[25] H. Knotz *et al.*, Appl. Phys. Lett. **88**, 241918 (2006).
[26] B. Das *et al.*, Phys. Rev. B **39**, 1411 (1989).